WP17ER-PR(18) 20999

M. Eisterer et al.

Predicting critical currents in grain-boundary limited superconductors

Preprint of Paper to be submitted for publication in
Physical Review B

This work has been carried out within the framework of the EUROfusion Consortium and has received funding from the Euratom research and training programme 2014-2018 under grant agreement No 633053. The views and opinions expressed herein do not necessarily reflect those of the European Commission.

Predicting critical currents in grain-boundary limited superconductors

M. Eisterer

Atominstitut, TU Wien, Stadionallee 2, 1020 Vienna, Austria

Abstract

The critical current across grain boundaries is severely suppressed in hight temperature superconductors, such as the cuprate or the iron-based compounds, if the grain boundary angle exceeds a few degrees. This is known from the low critical currents in untextured conductors and measurements on bi-crystalline films. Textured conductors were developed to overcome this limitation, however, a quantitative understanding between the degree of texture and the macroscopic critical current is still missing. A model for the prediction of the self-field critical current on the basis of experimental data obtained from bi-crystals is presented. It is a mean-field approach based on percolation theory. Without any fit parameter, good agreement with recent studies on cuprates and iron-based superconductors, where the critical current and the texture were analyzed quantitatively, is obtained. The simplified grain boundary physics hence describes the macroscopic properties of imperfectly textured materials.

I. INTRODUCTION

Many exciting superconducting materials have been discovered during the past decades. They are very promising for applications since they can significantly increase the operational space of superconductivity both in terms of temperature and magnetic field. The most promising among them, the cuprate and iron-based superconductors suffer from a bad connectivity between the grains of a conductor. It was shown on bi-crystalline films that the critical current across grain boundaries drops exponentially with the misalignment angle between the adjacent grains.[1, 2] The technological solution of this problem was the development of textured conductors, the most efficient form being coated conductors, where the grains are aligned within a few degrees so that they are sometimes called "single crystals by the mile". However, the according production processes are slow and expensive, hence the market is still dominated by NbTi and Nb_3Sn, which do not suffer from this granularity problem. Alternative texturing processes, in particular thermo-mechanical treatments, are cheaper although the resulting grain alignment is less perfect. Recent results on Bi-2212[3, 4] and Ba-122[5] indeed indicate the feasibility of this approach. The relation between texture and the macroscopic critical current density is still not understood quantitatively despite many approaches, such as the brick-wall,[6, 7] railway switch,[8], freeway[9], or parallel path[10] model, or various numerical approaches.[11–15] Most of them model the current meandering between the grains to predict the macroscopic behavior. Here, the approach is different, focusing on the statistical distribution of the grain boundary angles only and neglecting any details of the grain structure or its local variation. This enables a comparison of different materials on the basis of the experimentally observed dependence of the critical current density on misalgnement angle and a quantitative prediction of the influence of texture.

II. MEAN FIELD PERCOLATION MODEL

The percolation model is based on the mean field approach originally proposed for predicting the critical current density in MgB_2,[16] as well as its anisotropy upon texturing.[17] While the anisotropy of the upper critical field induces a variation of the properties of differently oriented grains and hence causes the inhomogeneity of the current flow in MgB_2,

the grain boundary currents are assumed to vary and limit per definition the macroscopic currents in grain-boundary limited superconductors. The critical current density, J_c, is obtained from a single integral[16]

$$J_c = \int_0^{J_c^{max}} \sigma_p dJ \tag{1}$$

with the effective cross section for current flow

$$\sigma_p = (\frac{p(J) - p_c}{1 - p_c})^t. \tag{2}$$

The percolation threshold, p_c is given by the minimal fraction of sites (grains) or bonds (grain boundaries) necessary for a continuous current path (spanning cluster). It is about 0.2 in three dimensional systems and depends on the coordination number, i.e. the number of neighboring grains. It is generally somewhat smaller in bond than in site percolation problems because removing one site removes all respective bonds, while a site may stay connected with the spanning cluster upon removing one of its bonds. For the sake of simplicity, $p_c = 0.2$ will be used in the following. The fraction of sites or bonds, $p(J)$, with J_c exceeding J is the only material dependent input, since the so-called transport exponent was fixed to 1.79. $p(J)$ is just $1 - F(J)$, with the distribution function of the critical current densities, $F(J_c)$. J_c^{max} is given by the condition $p(J_c^{max}) = p_c$ where the effective cross section becomes zero, because grain boundaries with higher critical current densities do not form a continuous cluster anymore and, therefore, cannot contribute more than J_c^{max} to the macroscopic current. The distribution function of the critical current density across grain boundaries has to be known or modeled in order to get the macroscopic critical current density by means of Equ.1. In principle, five parameters are needed to classify grain boundaries:

- The grain boundary angle
- The orientation of the rotational axis (2)
- The grain boundary plane (2)

A model for J_c as a function of all these five parameters is currently unavailable and we restrict our considerations to the grain boundary angle, α. Most available experimental data refer to [001] tilt boundaries (e.g. [1] and references therein) and an exponential decrease of

J_c as a function of α was found after a plateau at low angles in the cuprates[1] as well as in the iron-based superconductors[2]

$$J_c = J_0 e^{-1} \quad \text{for } \alpha \leq \alpha_c \tag{3}$$

$$J_c = J_0 e^{-\frac{\alpha}{\alpha_c}} \quad \text{for } \alpha \geq \alpha_c \tag{4}$$

Although the actual type of the grain boundary,[18] as well as its morphology[19] influence this dependence, the exponential behavior is a general trend in these two classes of superconductors and the critical currents across grain boundaries will modeled by Equs. 3 and 4. With this simplification, the distribution function of the grain boundary angle, α, has to be calculated to obtain $F(J_c)$ and $p(J)$ needed for the integral in Equ. 1.

A. Distribution of grain boundary angles

We first consider the angle distribution between two arbitrarily oriented grains. The orientation of one grain can be obtained by rotation of the other grain about the common axis. The rotation angle defines the grain boundary angle, α. For a total random orientation of both grains one obtains for $0 \leq \alpha \leq \pi$ (details are given in the Appendix)

$$f(\alpha) = \frac{1 - \cos\alpha}{2\pi} \tag{5}$$

$$F(\alpha) = \frac{\alpha - \sin\alpha}{2\pi} \tag{6}$$

$f(\alpha)$ denotes the distribution density of the distribution function $F(\alpha)$, i.e. $f(\alpha) = F'(\alpha)$. The angular range is restricted to 180° since clockwise and anticlockwise rotations result in the same boundary. However, we have further symmetries because a rotation about 180° results in the same crystal lattice. We further assume that the effect of orthorhombicity is small, hence rotations about the crystallographic c-axis have a periodicity of 90°. This leads to

$$F(\alpha) = \frac{8}{\pi}(\alpha - \sin\alpha) \tag{7}$$

for $\alpha \leq \frac{\pi}{4}$,

$$F(\alpha) = 2 - \frac{8}{\pi}(\cos\alpha + 1)\tan\frac{\pi}{8} \tag{8}$$

for $\frac{\pi}{4} \leq \alpha \leq \frac{\pi}{2}$, and approximately

$$F(\alpha) \approx 2 - \frac{4}{\pi}\arccos(2\cos\alpha + 1) - \frac{8}{\pi}(\cos\alpha + 1)(\tan\frac{\pi}{8} - \tan\frac{\arccos(2\cos\alpha + 1)}{2}) \tag{9}$$

for $\frac{\pi}{2} \leq \alpha \leq 1.7178$. The distribution function (bottom panel) and the distribution density (top panel) are shown as gray lines in Fig.1. The circles in the figure were obtained from numerical simulations assuming cubic grains on a simple cubic lattice. The orientation of the grains was chosen randomly and the distribution function and density were obtained by counting the grain boundary angles in a small angular range. Details are given in the Appendix. These simulations are necessary to obtain the distribution of grain boundary angles in textured samples, as well as to ensure that the distribution is also valid for a large ensemble of grains. The analytical expressions are valid for the distribution of two grains with random orientation, but the grain boundary angles are not independent of each other in a large ensemble, which becomes evident by considering a closed path. The grain boundary angles are restricted by the condition that the grain orientation has to be the same after the entire loop. Although this restriction does not change the angular distribution in an ensemble of randomly oriented grains, it does for partially aligned grains (not shown) and the maximum in the distribution function for the ensemble shifts to lower angles compared to the case of two grains. The differences between the analytical formula and the simulation at grain boundaries above 90° is caused by another reason: the derivation of the formula does not take all symmetries into account (cf. Appendix). A first important result follows from the grain boundary angle distribution between randomly oriented grains. The distribution function becomes 0.2, which is a typical percolation threshold in three-dimensional materials, only at about 45° (upper panel in Fig. 1). Since nearly all experimental data for critical currents across grain boundaries were obtained for bi-crystals with misorientation anlges up to 45°,[1] these data are not useful for predicting the behavior of untextured materials. If the fraction of grain boundaries with angles below 45° is smaller than the percolation threshold, these boundaries can per definition not form a continuous current path throughout the entire sample and consequently not contribute more to the global currents than the best links in the remaining matrix. Data for grain boundaries with grain boundary angles above 45° are needed for this purpose. We will restrict our considerations in the following to textured samples, where the grain boundaries below 45° determine the properties so that the available experimental data can be used.

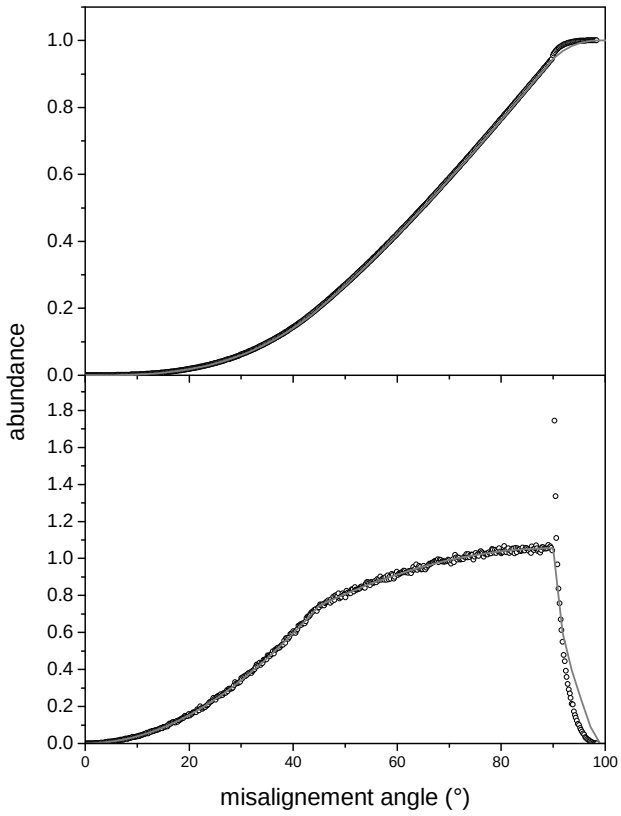

FIG. 1: Distribution function (upper panel) and distribution density (lower panel) of grain boundary angles in randomly oriented grains. The line graphs were obtained from the analytical expressions (cf. Equs. 7-9), the circles represent the results from the simulation.

B. Preferred grain orientation

A Gaussian distribution density of the grain misalignment from the preferred orientation is assumed

$$f(\theta) \;\propto\; e^{-\frac{\theta^2}{2\theta_\mathrm{t}^2}} \sin\theta \tag{10}$$

$$f(\phi) \;\propto\; e^{-\frac{\phi^2}{2\phi_\mathrm{t}^2}} \tag{11}$$

where ϕ_t and θ_t quantify the in- and out-of-plane texture, respectively. With this definition, the full width at half maximum (FWHM) is larger by a factor of $2\sqrt{2\ln 2} \approx 2.35$ than these texture angles.

The upper panel in Fig. 2 shows the evolution of the grain boundary angle distribution density with texture for pure out-of-plane texture, as achieved for instance by thermo-mechanical treatments (see Bi-2223 below). With decreasing θ_t, a peak evolves below 90°

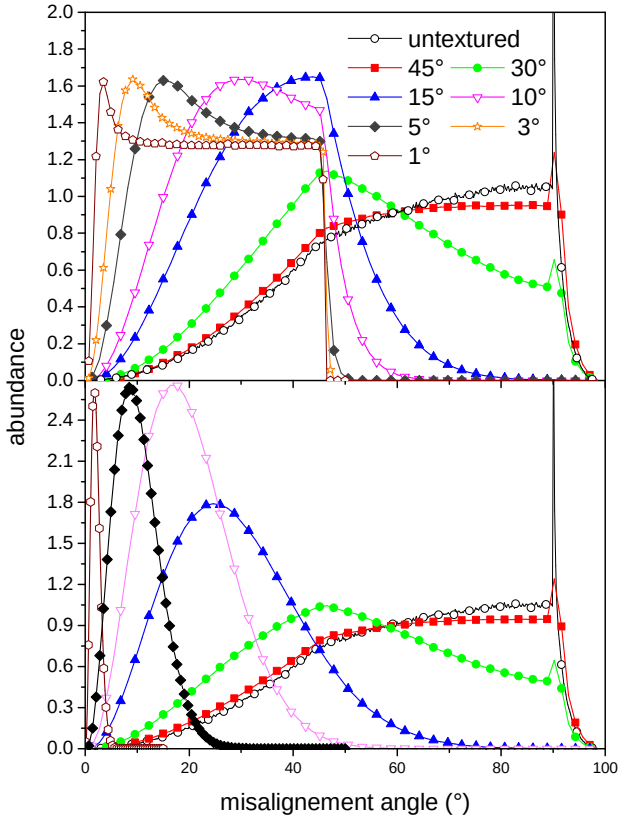

FIG. 2: Distribution density of the grain boundary angles for uni- (upper panel) and bi-axial (lower panel) texture. The given angles refer to the out-of-plane texture angle, θ_t. $\phi_t = \theta_t$ is assumed for bi-axial texture, $\phi_t = \infty$ for uniaxial texture. The distribution densities were divided by 2 and 5 for $\phi_t = 5°$ and 1°, respectively, to fit into the lower panel.

and shifts to lower angles upon improving texture. A plateau develops below 45° which finally extends to 0° in the limit $\theta_t = 0$ when the peak disappears reflecting the equal distribution of the in-plane misorientation anlge, ϕ.

This plateau does not occur for biaxial texture. The distribution densities displayed in the lower panel of Fig. 2 were calculated for $\phi_t = \theta_t$ meaning the same in- and out-of-plane alignment. There is hardly any difference to uni-axial texture at $\theta_t = 45°$, some weight is transfered to grain boundary angles below 45° at $\theta_t = 30°$ and the peak shifts from 45° to about 25° for $\theta_t = 15°$, becoming more symmetric for bi-axial grain alignment. At lower texture angles, the distribution functions become very different, because of the absence of the plateau. The distribution density has to converge to the delta function for $\theta_t = \phi_t \to 0°$.

We will restrict our considerations in the following to textured samples with texture

angles below 15°, where grain boundaries below 45° determine the properties so that the available experimental data can be used. Figure 3 demonstrates the influence of texture on J_c. The open and solid symbols refer to uni- ($\phi_t = \infty$) and bi-axial ($\phi_t = \theta_t$) texture. The decay angle, α_c, in Equ. 4 was chosen 5 and 9, as representative for cuprate and iron-based superconductors.[1, 2] . The upper pannel represents the suppression of J_c, the data are normalized by J_0/e (cf. Equ. 4). In case of uniaxial texture, a plateau is found at low angles in both materials, where the in-plane misorientation dominates. A large decay angle, α_c, in Equ. 4 is crucial for large currents in case of pure out-of-plane texture. The currents are suppressed to 9% and 1.5% for perfect out-of-plane textrue ($\theta_t = 0$) in the iron-based ($\alpha_c = 9°$) and cuprate ($\alpha_c = 5°$) superconductors, respectively. The low-angle plateau is restricted to very small angles in case of bi-axial texure, when all misorientation angles are below α_c and the grain boundaries do not limit the currents anymore. If the texture becomes weaker, α_c determines the slope of the approximately exponential decrease in J_c with θ_t for both, uni- and bi-axial texture.

The positive effect of the larger α_c in the iron-based superconductors, is partly compensated by a smaller J_0. For instance, J_0 was reported to be $2.8 \cdot 10^6$ Acm^{-2} for Co-doped Ba-122 and the data for YBCO summarized in Fig. 30 of the review from Hilgenkamp und Manhart can be described by $J_0 = 2 \cdot 10^7$ Acm^{-2}. Much less data obtained from bi-crystals are available for other compounds of these superconducting families. Since the properties of BiSSCO and K-doped Ba-122 tapes and wires will be discussed later, J_0 of these compounds has to be estimated. The maximum current density that can be obtained in superconductors scales with the depairing current density J_d, it seems hence reasonable to re-scale J_0 with the respective depairing current densities, which are about 400, 240, 110, and 75 MAcm^{-2} in YBCO, BiSCCO (similar for 2212 and 2223), K- and Co-doped Ba-122, respectively. This leads to $J_0 \approx 1.25 \cdot 10^7$ Acm^{-2} for BiSCCO 2212 and 2223 and $J_0 \approx 6.35 \cdot 10^6$ Acm^{-2} for K-doped Ba-122. These data refer to low temperatures (around 4.2 K) and self-field. The resulting current densities are shown in the lower panel of Fig. 3. Iron-based superconductors are favorable against the cuprates for uni-axially textured conductors under the viewpoint of required grain alignment. The situation is more complex in bi-axially textured conductors where the cuprates (BiSSCO) reach higher currents at high texture crossing below J_c of K-doped Ba-122 at around $\theta_t = 5°$. The situation is even more favorable for YBCO, since its J_d and hence J_0 are higher.

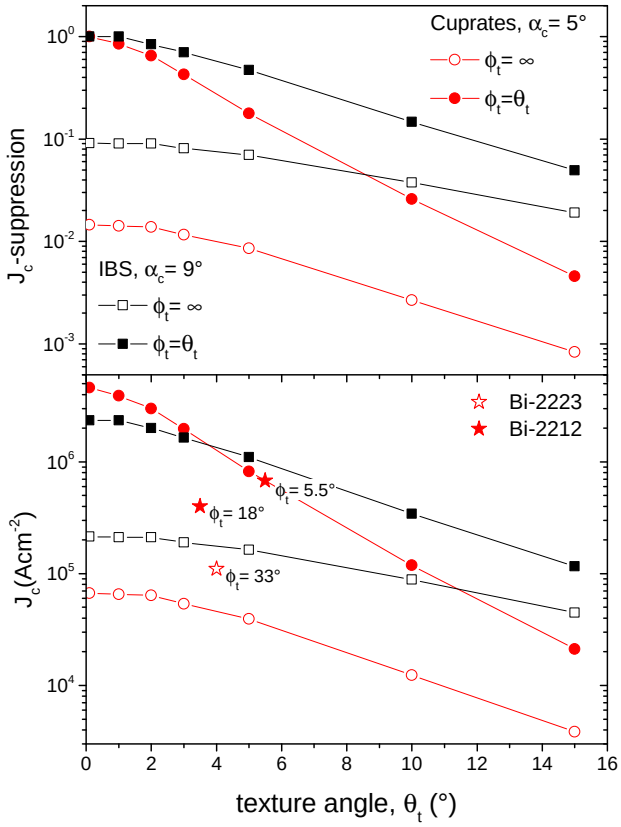

FIG. 3: Critical current densties as a function of texture quantified by θ_t. The current densities are normalized to the intraganular value (i.e. α=0) in the upper panel. The expected values of J_0 for Bi-2212/2223 and K-doped Ba-122 were used to calculate the current densities shown in the lower panel.

III. COMPARISON WITH EXPERIMENTAL DATA

The excellent work of Kametami et al.[20] provides data on texture obtained from Electron Backscatter Diffraction Orientation Imaging Microscopy (EBSD-OIM) together with critical current densities of the same conductor. This is ideal to check the predictions of the calculations and to validate the underlying, simplified grain boundary physics. The upper panel in Fig. 4 compares the experimentally obtained distribution density of the grain boundary angles in a Bi-2223 tape with the theoretical expectation. The gray line corresponds to pure out-of-plane texture. The experimental data do not show this plateau-like behavior, or the peak is much higher than the plateau, hence the in-plane orientation is likely not totally random. This is taken into account by adding a weak in-plane alignment ($\phi_t = 33°$), which

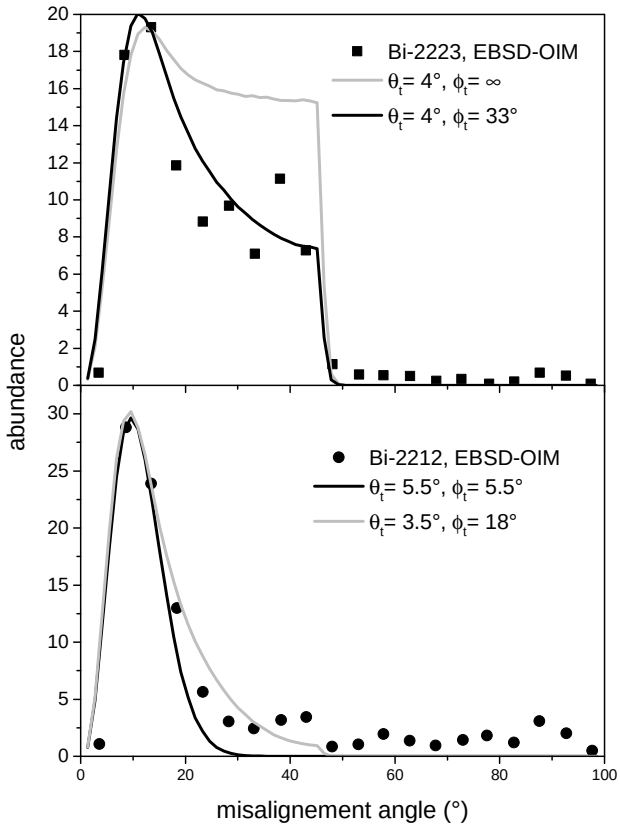

FIG. 4: Distribution density of grain-boundary angles in Bi-2223 tapes (upper panel) and Bi-2212 wires (lower panel) . Experimental data (symbols) were extracted from Ref. [20].

leads to a much better agreement with the experiment (black line). The lower panel refers to a Bi-2212 wire, where a local texture enables a high critical current. The experimental data can be reasonable described by a similar in- and out-of-plane texture of about 5.5°, or assuming a high out-of-plane texture (3.5°) and a weaker in-plane alignment. The latter is supported by the step at 45° in the experimental data. However, the plateau between 5.5° and 5.5° cannot be described either way. This in turn leads to the conclusion, that the Gaussian distribution of the grain boundary angle is a useful approximation for Bi-2212 and 2223, but does not rigorously apply.

The critical current densities predicted on the basis of these distribution densities are represented by the stars in the lower panel of Fig. 3. $4 \cdot 10^5\,\mathrm{Acm}^{-2}$ are obtained with $\theta_\mathrm{t} = 3.5°$, $\phi_\mathrm{t} = 18°$ and $\theta_\mathrm{t} = 5.5°$, $\phi_\mathrm{t} = 5.5°$ result in $6.8 \cdot 10^5\,\mathrm{Acm}^{-2}$. The latter value is in excellent agreement to the experimental data, about $6 \cdot 10^5\,\mathrm{Acm}^{-2}$ were reported for the Bi-2212 wire at 1 T, the lowest field data are available.[20] The model somewhat underestimates

the current density in the Bi-2223 tape. It predicts $1.1 \cdot 10^5\,\mathrm{Acm}^{-2}$ for $\theta_\mathrm{t} = 4°$, $\phi_\mathrm{t} = 33°$, while the self-field J_c of the tape is certainly above $2 \cdot 10^5\,\mathrm{Acm}^{-2}$ (experimental data are available only for fields down to 2 T).

Another study on grain alignment and the resulting J_c is available for K-doped Ba-122.[5]. The distribution density of the grain boundary angles given in Fig. 5 of that paper cannot be described well by the Gaussian distributions 10 and 11. Therefore, the data of the bar graph were extracted and linearly interpolated for the calculations, which predict a J_c of $4.4 \cdot 10^5\,\mathrm{Acm}^{-2}$. This value cannot be compared to experimental data directly, since only high field data are available at low temperature. The behavior of the volume pinning force $F_\mathrm{p} = J_\mathrm{c}B \propto b^{0.64}(1-b)^{2.3}$ observed at high temperatures[5] was hence used to extrapolate the high field data to self field, which was estimated self-consistently from $B^\mathrm{self} \approx \mu_0 J_\mathrm{c} d/2$ with the sample thickness d: $J_\mathrm{c} \approx 4.8 \cdot 10^5\,\mathrm{Acm}^{-2}$.

Untextured, polycrystalline materials cannot be modeled because the behavior of J_c across grain boundaries with misalignment angles above 45° is unknown. However, by looking on the data of Katase et al.[2] (Fig. 1b), it is tempting to speculate that $J_\mathrm{c}(\theta_\mathrm{GB})$ becomes constant above 30° since the values at 30° and 45° are very similar. With this assumption about high angle grain boundaries our approach would predict a current density of $2.2 \cdot 10^5\,\mathrm{Acm}^{-2}$ while the highest reported self-field J_c is around $1.2 \cdot 10^5\,\mathrm{Acm}^{-2}$.[21]

IV. DISCUSSION

The agreement between the model and the experimental data is astonishing, given the various assumptions and simplifications, in particular the reduction of the grain boundary properties to one parameter and the Gaussian distribution of the grain orientation. Note that there is no free parameter, since all parameters ($J_\mathrm{d}, J_0, \alpha_\mathrm{c}, p_\mathrm{c}$) were fixed in accordance with literature values before the calculations. The behavior of the grain boundaries are based on experiments on PLD (pulsed laser deposition) films on bi-crystalline substrates, which may or may not be representative for natural grain boundaries. Even in these films the scatter of data is considerable. Also no common agreement on the values of the depairing current density, J_d, (or superfluid density) of the various materials has been reached so far. Since the parameter selection was subjective (but not biased in view of the results) some coincidence is certainly responsible for the agreement and a discussion of quantitative

differences is pointless. There are good reasons that the approach overestimated the critical currents in polycrystalline conductors: The superconducting matrix is assumed to be perfect (no voids, secondary phases etc.) and the average self-field is certainly smaller at the artificial grain boundaries than in the conductors under consideration. On the other hand, there a good reasons for the opposite as well: The critical current density along the very planar grain boundaries resulting from PLD are smaller than those across meandering grain boundaries,[19] which often arise from other synthesis techniques. Percolating currents could preferentially cross grain-boundaries under reduced Lorentz force, and last but not least the large aspect ratio of the grains in particular in the BiSCCO compounds could enable a much higher macroscopic (longitudinal) current density than the local (mainly transversal) inter-grain current densities[22] (cf. brick wall model[6, 7]).

The model is restricted so far to the self-field limit and to textured materials mainly because of the availability of data on grain boundary currents. The extension to untextured materials or materials containing a significant fraction of grain boundaries with misalignment angles above 45° is straight forward when the according experimental data or theoretical predictions become available. Predicting in-field currents might be more complex, because the orientation of the local field with respect to the grain boundary becomes of importance and is hard to address within this approach.

V. CONCLUSIONS

A model for the quantitative prediction of the macroscopic critical currents based on experimental data for the texture and grain boundary properties was developed and successfully applied to Bi-2212 tapes, Bi-2212 wires and Ba-122 tapes. The good agreement between prediction and experiment indicate that the simplified grain boundary physics covers the essential physics of imperfectly textured high temperature superconductors. For (perfect) uniaxial texture (out-of-plane), the currents are suppressed to 9% and 1.5% compared to highly biaxially textured materials in the iron-based and cuprate superconductors, respectively. A reliable prediction for untextured materials is not possible, because the relevant grain boundaries have a misorientation above 45 in that case and only very few experimental data exist for such high angle grain boundaries.

VI. APPENDIX

A. Grain boundary angle between two adjacent grains

Without loss of generality, the crystallographic axes of the first grain are assumed to be parallel to the x-, y-, and z-axes of the Cartesian coordinate system. The crystallographic axes of the other grain can be considered as the axes of another coordinate system and the unit vectors of $\vec{a}$, $\vec{b}$, and $\vec{c}$ define the transformation matrix between these two coordinate systems

$$T = \begin{pmatrix} - & \vec{e_a} & - \\ - & \vec{e_b} & - \\ - & \vec{e_c} & - \end{pmatrix} \tag{12}$$

T then also defines the rotation of the two crystallographic lattices and the rotation angle can be easily obtained from

$$\mathrm{trace}(T) = 1 + 2\cos\alpha \tag{13}$$

The rotation axis is the eigenvector of T to the eigenvalue 1.

B. Distribution of grain boundary angles

We start with perfectly aligned grains (i.e. $\alpha = 0$), their (normalized) crystallographic axes defining our coordinate system. In order to change the orientation of the second grain, we first establish its in-plane misorientation by a rotation about $\vec{e_z}$ (or $\vec{e_c}$)

$$R_{\mathrm{in}} = \begin{pmatrix} \cos\phi_{\mathrm{in}} & -\sin\phi_{\mathrm{in}} & 0 \\ \sin\phi_{\mathrm{in}} & \cos\phi_{\mathrm{in}} & 0 \\ 0 & 0 & 1 \end{pmatrix} \tag{14}$$

The out-of-plane misorientation is then defined by the orientation of $\vec{c}$ with its unit vector

$$\vec{e_c} = \begin{pmatrix} \sin\theta\cos\phi \\ \sin\theta\sin\phi \\ \cos\theta \end{pmatrix} \tag{15}$$

θ defines the out-of-plane misorientation angle. To obtain $\vec{e_c}$ from $\vec{e_z}$ and keep the in-plane misorientation unaltered, the second grain has to be rotated about $\vec{n} = \vec{e_z} \times \vec{e_c}/|\vec{e_z} \times \vec{e_c}| =$

$(-\sin\phi, \cos\phi, 0)^T$. The corresponding rotation matrix is given by

$$R_{\text{out}} = \begin{pmatrix} n_1^2(1-\cos\theta) + cos\theta & n_1 n_2(1-\cos\theta) - n_3\sin\theta & n_1 n_3(1-\cos\theta) + n_2\sin\theta \\ n_1 n_2(1-\cos\theta) + n_3\sin\theta & n_2^2(1-\cos\theta) + cos\theta & n_2 n_3(1-\cos\theta) - n_1\sin\theta \\ n_1 n_3(1-\cos\theta) - n_2\sin\theta & n_2 n_3(1-\cos\theta) + n_1\sin\theta & n_3^2(1-\cos\theta) + cos\theta \end{pmatrix} \tag{16}$$

The rotation (or misalignment) angle can be calculated from Equ. 13 with $T = R_{\text{out}} R_{\text{in}}$

$$\cos\alpha = \frac{1}{2}(\cos\theta + \cos\theta\cos\phi_{\text{in}} + \cos\phi_{\text{in}} - 1) \tag{17}$$

For a random orientation, ϕ_{in} is equally distributed on $[0\ 2\pi]$ (i.e. $f(\phi_{\text{in}}) = 1/2\pi$) and θ is distributed as $f(\theta) = \frac{1}{2}\sin\theta$ on $[0\ \pi]$. The distribution function for α is obtained by calculating the fraction of grains with a misalignement angle less than or equal to α. ϕ_{in} can vary between 0 and α, and $\cos\theta$ is, for a given α and ϕ_{in}, restricted by Equ. 17

$$F(\alpha) = \int_0^{\alpha} \frac{1}{2\pi} d\phi_{\text{in}} \int_0^{\arccos\frac{2\cos\alpha - \cos\phi_{\text{in}} + 1}{1+\cos\phi_{\text{in}}}} \frac{1}{2}\sin\theta d\theta = \frac{1}{2\pi}(\alpha - \sin\alpha) \tag{18}$$

If θ and ϕ_{in} are restricted to $\pi/2$ and $\pi/4$, respectively, the maximum misalignement angle becomes $\alpha_{\max} = 1.7178 = 98.42°$ and the distribution functions 7-9 are obtained.The different angular regions result from the changing limits of the integration over ϕ_{in}: the upper limit is fixed to $\pi/4$ for $\alpha > \pi/4$, the lower limit becomes larger than zero for $\alpha > \pi/2$.

Since it turned out to be difficult to derive analytical expression for non-random grain orientations, numerical simulations were performed. Cubic grains (typically about 150^3) were arranged on a simple cubic lattice (coordination number of 6). Their orientation was chosen as outlined above (in- and out-of-plane rotation), but allowing a preferred grain orientation according to Equs. 10 and 11 if desired. The coordinate system of the first grain is transformed into the system of the other grain by $T = T_2^T T_1$ where T_1 and T_2 are the rotation matrices of the two grains defined as above ($T = R_{\text{out}} R_{\text{in}}$). The rotation angle is then in principle obtained from relation 13. However, the symmetries has to be taken into account which results in

$$\cos\alpha = \frac{1}{2}(\max(|T_{1,1}| + |T_{2,2}|, |T_{1,2}| + |T_{2,1}|) + |T_{3,3}| - 1) \tag{19}$$

The absolute value reflect inversion symmetry, the maximum refers to an exchange of the *a*- and *b*-axes. The grain boundary angles of all pairs of grains are calculated and assigned to the respective angular interval to derive the distribution density.

Acknowledgments

I wish to thank Harald W. Weber for critically reading this paper. This work has been carried out within the framework of the EUROfusion Consortium and has received funding from the Euratom research and training programme 2014-2018 under grant agreement No 633053. The views and opinions expressed herein do not necessarily reflect those of the European Commission.

---

[1] H. Hilgenkamp and J. Mannhart, Rev. Mod. Phys. **74**, 485 (2002).

[2] T. Katase, Y. Ishimaru, A. Tsukamoto, H. Hiramatsu, T. Kamiya, K. Tanabe, and H. Hosono, Nat. Comm. **2**, 409 (2011).

[3] D. C. Larbalestier, J. Jiang, U. P. Trociewitz, F. Kametani, C. Scheuerlein, M. Dalban-Canassy, M. Matras, P. Chen, N. C. Craig, P. J. Lee, et al., Nat. Mater. **13**, 375 (2014).

[4] I. Pallecchi, A. Leveratto, V. Braccini, V. Zunino, and A. Malagoli, Supercond. Sci. Technol. **30**, 095005 (2017), URL `http://stacks.iop.org/0953-2048/30/i=9/a=095005`.

[5] H. Huang, C. Yao, C. Dong, X. Zhang, D. Wang, Z. Cheng, J. Li, S. Awaji, H. Wen, and Y. Ma, Supercond. Sci. Technol. **31**, 015017 (2018), URL `http://stacks.iop.org/0953-2048/31/i=1/a=015017`.

[6] L. N. Bulaevskii, J. R. Clem, L. I. Glazman, and A. P. Malozemoff, Phys. Rev. B **45**, 2545 (1992), URL `https://link.aps.org/doi/10.1103/PhysRevB.45.2545`.

[7] L. N. Bulaevskii, L. L. Daemen, M. P. Maley, and J. Y. Coulter, Phys. Rev. B **48**, 13798 (1993), URL `https://link.aps.org/doi/10.1103/PhysRevB.48.13798`.

[8] B. Hensel, G. Grasso, and R. Flükiger, Phys. Rev. B **51** (1995), URL `https://link.aps.org/doi/10.1103/PhysRevB.51.15456`.

[9] G. N. Riley, A. P. Malozemoff, Q. Li, S. Fleshler, and T. G. Holesinger, JOM **49**, 24 (1997), URL `https://doi.org/10.1007/BF02914734`.

[10] D. C. van der Laan, J. Schwartz, B. ten Haken, M. Dhallé, and H. J. N. van Eck, Phys. Rev. B **77**, 104514 (2008), URL `https://link.aps.org/doi/10.1103/PhysRevB.77.104514`.

[11] E. D. Specht, A. Goyal, and D. M. Kroeger, Phys. Rev. B **53**, 3585 (1996).

[12] R. Haslinger and R. Joynt, Phys. Rev. B **61**, 4206 (2000).

[13] E. E. Specht, A. Goyal, and D. M. Kroeger, Supercond. Sci. Technol. **13**, 592 (2000), URL http://stacks.iop.org/0953-2048/13/i=5/a=331.

[14] Y. Nakamura, T. Izumi, and Y. Shiohara, Physica C **371**, 275 (2002).

[15] B. B. Zeimetz, B. A. Glowacki, and J. E. Evetts, Eur. Phys. J. B **29**, 359 (2002).

[16] M. Eisterer, M. Zehetmayer, and H. W. Weber, Phys. Rev. Lett. **90**, 247002 (2003).

[17] M. Eisterer, W. Häß ler, and P. Kováč, Phys. Rev. B **80**, 174516 (2009).

[18] R. Held, C. W. Schneider, J. Mannhart, L. F. Allard, K. L. More, and A. Goyal, Phys. Rev. B **79**, 014515 (2009).

[19] D. M. Feldmann, T. G. Holesinger, R. Feenstra, C. Cantoni, W. Zhang, M. Rupich, X. Li, J. H. Durrell, A. Gurevich, and D. C. Larbalestier, Journal of Applied Physics **102**, 083912 (pages 5) (2007), URL http://link.aip.org/link/?JAP/102/083912/1.

[20] F. Kametani, J. Jiang, M. Matras, D. Abraimov, E. E. Hellstrom, and D. Larbalestier, Sci. Rep. **5**, 8285 (2015).

[21] J. D. Weiss, C. Tarantini, J. Jiang, F. Kametani, A. A. Polyanskii, D. C. Larbalestier, and E. E. Hellstrom, Nat. Mater. **11**, 682 (2012).

[22] G. Hammerl, A. Herrnberger, A. Schmehl, A. Weber, K. Wiedenmann, C. W. Schneider, and J. Mannhart, Appl. Phys. Lett. **81**, 3209 (2002).